SUBMILLIMETER OPTICAL PROPERTIES OF HEXAGONAL BORON NITRIDE

A. J. Gatesman, R. H. Giles and J. Waldman

Department of Physics and Applied Physics

University of Massachusetts Lowell

Lowell, MA 01854

ABSTRACT

The submillimeter optical properties of hot-pressed polycrystalline boron nitride with a predominantly hexagonal crystal structure were studied at room temperature from approximately 20 cm^{-1} to 120 cm^{-1} (λ = 500 μm - 84 μm) with a Fourier transform spectrometer. Several grades were studied and probed both parallel and perpendicular to the material's optic axis. The material was found to behave as a negatively uniaxial birefringent crystal. The birefringence, defined as the difference between the real part of the extraordinary and ordinary indices of refraction (n_e - n_o), was quite large in one case with a value of -0.152. The material's absorption properties were also studied. For certain grades, a modest dichroism was observed. The low absorption (α < 1 cm^{-1}) for grade A at frequencies below 38 cm^{-1} suggests the possibility for millimeter/submillimeter wave applications. Results are compared with data obtained by other researchers on related materials.

INTRODUCTION

Boron nitride (BN) has received considerable attention within the last few years due to its favorable mechanical, electrical, optical and chemical properties over a wide range of temperatures. This material is used in applications such as transmitting substrates for X-ray lithography masks, high quality insulating films for metal-insulator-superconductor (MIS) structures, and coatings to increase the hardness of materials.[1] Boron nitride has previously been studied in the ultraviolet, optical, infrared, and microwave frequencies.[2,3,4] Its low absorption coefficient in the microwave has made BN a candidate for window material for gyrotrons, free electron lasers and reentry vehicle communication systems.[4,5] BN crystallizes in two forms: cubic (zinc blende) and hexagonal structures. BN films grown by processes such as chemical vapor deposition and sputtering have the cubic crystal structure (similar to that of GaAs).   The material used in this study was hot-pressed BN where the raw material is subjected to a high uniaxial compressive force at an elevated temperature. This results in an orderly arrangement of the boron and nitrogen atoms (a structure similar to that of graphite, see Figure 1). The resulting material is *not*, however, single crystal, but a highly oriented polycrystalline material. This paper reports the optical properties of hot-pressed hexagonal BN (*h*-BN) in the submillimeter region of the spectrum.

A material with a hexagonal crystal structure is known to be optically anisotropic with a single optic axis coinciding with the axis of crystal symmetry.[6] In this case, the dielectric constant ε is a 3 x 3 tensor. The dielectric tensor can be shown to be symmetric[7] and the nine components reduce to six where $\varepsilon_{ij} = \varepsilon_{ji}$ for $j \neq i$. Furthermore, there exists an orientation of the Cartesian coordinate system where its axes are aligned with the material's preferred axes (i.e., in the hexagonal case, one of the Cartesian axes aligned with the optic axis). This coordinate system is referred to as the principal set of axes and the six components of ε reduce to three (ε_x, ε_y, ε_z) where the off diagonal elements are zero.

With the Cartesian coordinate system aligned along the material's preferred axes as in Figure 1, $_y$ will equal $_z$ due to the degree of symmetry inherent in the hexagonal crystal structure. In this case, the x-axis is the axis of symmetry (the optic axis) and the planes of atoms are in the y-z plane. This leaves the dielectric constant (or equivalently the complex refractive index, n - ik, where n and k are the real and imaginary parts, respectively) to be determined for just *two* cases: (1) the electric field parallel to the x axis and (2) the electric field in the y-z plane.

Hot pressed hexagonal boron nitride was obtained in four grades (A, HP, M, M26) in 2" diameter discs and approximately 1 mm thickness from The Carborundum Company in Niagara Falls, NY. Two samples per grade were provided: one whose flat surface was parallel to the crystal planes and one whose flat surface was perpendicular to the crystal planes. With a controlled incident linear state of polarization, the response of both parallel and perpendicular directions to the optic axis could be probed.

EXPERIMENTAL

The optic axis of the parallel cut samples is obviously normal to the sample surface. For normally incident radiation, these disks were expected to behave as optically isotropic materials. The optic axis of the perpendicularly cut samples lay somewhere along a diameter and had to be located. This direction was determined by transmitting submillimeter radiation (513 μm) from an optically pumped molecular gas laser through the disc which was situated between two wire grid linear polarizers whose wires were oriented perpendicular to one another. Two orthogonal axes in the plane of the *h*-BN (one of them being the optic axis) could then be found by rotating the disc along the axis of propagation to produce a null at the detector. This procedure allowed for the determination of the two orthogonal axes in the plane of each perpendicularly cut sample

to within approximately two degrees.

In order to distinguish the optic axis, a Fourier transform spectrometer was employed from 18 cm^{-1} to 118 cm^{-1}. Our instrument has been optimized for long wavelength data collection and employs a liquid helium cooled silicon bolometer. Data was collected with a resolution of 0.1 cm^{-1}. A pair of wire grid linear polarizers configured with their wires parallel were positioned in front of the *h*-BN to insure a well defined linear state incident on the material. Twelve spectra were collected in total. The first four were grades A, HP, M and M26 in the parallel orientation. The remaining eight were the four grades with the optic axis parallel and then perpendicular to the incident linearly polarized radiation. The transmission spectra for grades A and M26 in the perpendicular orientation are shown in Figure 2. Spectra for grades HP and M in the perpendicular orientation are similar to (but not identical) to the M26 spectra and are not shown. The spectra of the parallel cut samples are not shown as they were nearly identical to one of the two perpendicularly cut samples (as expected) and were useful only in determining which axis was the extraordinary (optic) axis and which one was the ordinary axis. Grade A is interesting because of its lower loss and M26 is interesting because of its dichroic behavior. Both of these points will be returned to later in the Results and Discussion section.

Derivation of the Optical Properties

The material's refractive index n, and absorption coefficient , were both determined from the transmissivity data. Characteristic of all of the spectra is the rapid oscillation which is caused by the interference between the front and back surfaces of the sample (channel spectra). A transmission maximum occurs when an integral number of wavelengths within the material equals twice the thickness t:

$$m \ _n = 2t,$$

where λ is the vacuum wavelength, λ_n equals λ/n and $m = 0, 1, 2, 3,...$ or written another way:

$n = \dfrac{m}{2\,\nu\,t}$ where ν is the frequency in cm^{-1}. The thickness of the samples were measured with an uncertainty of ±0.0001" (±3µm). With the order number and location in frequency of each of the maxima determined, a value of n could then be associated with each peak of the spectra. Values of n for the extraordinary (optic) axis and perpendicular to it (ordinary axis) are given in Figure 3 and are labelled n_e and n_o respectively. The uncertainty in n (Δn) is ± 0.006 and is due primarily to the uncertainty in the material's thickness (Δt/t ≈ 0.003).

Calculation of the material's absorption coefficient, α, as a function of frequency was performed in the following way. First realize that the transmissivity T through a homogeneous etalon of uniform thickness is a function of the complex index of refraction, thickness and the wavelength;

$$T_{expt} = f(n, k, t, \lambda).$$

For each peak in the spectra, n, t, λ and T_{expt} are known. This leaves a single unknown, k, to be determined ($\alpha = 4\pi k/\lambda$). A value of k at a given peak is found by increasing k from 0 until a modelled value of the transmissivity (T_{model}) using the appropriate n, t and λ, matches the experimental value. Values of the absorption coefficient α are given for the four grades in Figure 4.

The uncertainty in α is difficult to calculate because it cannot be solved analytically in terms of T_{expt}, n, λ, and t. However, since the major source of error in α is the uncertainty in T_{expt}, $\Delta\alpha$ can be estimated in the following manner. The accuracy of the transmissivity data is 0.02. After a value of k is found at a particular peak that reproduces the data, it is then varied again (either higher or lower) until $|T_{model} - T_{expt}| > 0.02$. This value of k is called k_{error} and an estimate in the uncertainty in k is given by $|k - k_{error}|$. The corresponding uncertainty in α is indicated by the vertical error bars on two data points in each of the plots. Two bars are given to indicate any slow changes in the uncertainty with frequency.

RESULTS and DISCUSSION

The birefringence for all grades was found to be roughly constant in the frequency range studied. Values of n were -0.108, -0.098, -0.065, and -0.152 for grades A, HP, M, and M26 respectively. Optical properties of related materials also show a strong birefringence. Aluminum oxide (Al_2O_3), also known as sapphire, crystallizes in the rhombohedral structure. Because of this crystal structure, it is also uniaxially birefringent. The birefringence is evident in the visible and increases into the millimeter range.[8] Barker[9] has measured optical properties of Al_2O_3 from 1 to 140 μm and fitted his reflection spectra with the dielectric-function model:

$$\varepsilon = \varepsilon_\infty + \sum_j \frac{\varepsilon_j \omega_j^2}{\omega_j^2 - \omega^2 + i \gamma_j \omega}. \tag{1}$$

ε is the complex dielectric constant and ε_∞ is the dielectric constant at frequencies higher than all lattice modes but below electronic contributions. ε_j, ω_j, and γ_j are the oscillator strength, frequency and damping of the jth transverse optic mode respectively. Using these data, Ref. 8 has calculated n and k for the electric field parallel and perpendicular to the material's (optic) c-axis. For comparison, the birefringence and dichroism of h-BN, Al_2O_3, and BeO at 100 cm^{-1} are given in Table I.

Using the above technique to calculate optical properties is not necessary in the SMM. The absorption coefficient of typical insulators drop rapidly with frequency in this region. In the case of h-BN, the absorption coefficient, α decreases by about one order of magnitude between 100 cm^{-1} and 20 cm^{-1}. Reflection spectra are therefore not necessary and the optical properties can be completely determined by analyzing the transmission channel spectra as described earlier.

Another material demonstrating strong birefringent behavior which has been studied in the far-infrared is Beryllium oxide (BeO). Loh[10] has studied the lattice vibrations of this uniaxial

material by measuring the polarized spectra of both the infrared reflectance and Raman scattering on single crystals at room temperature. He then derived optical constants from the reflection spectra by best fit with parameters in a dispersion formula of a classical oscillator similar to equation (1). Ref. 8 extended the calculation to 100 cm^{-1} in order to estimate the static dielectric constant. Values of the birefringence and dichroism for BeO are also given in Table I.   One difference between these materials and h-BN is that h-BN exhibits a negative birefringence.

All grades of h-BN studied were found to exhibit dichroic behavior to some degree as can be seen in Figure 4. In grades A, M, and M26, the dichroism ($\Delta\alpha$ = α_e - α_o) is seen to be frequency dependent with increasing values towards shorter wavelengths. Grade HP is the only exception with $\Delta\alpha$ barely larger than the uncertainty at the longest wavelengths studied. In all cases the absorption measured for the electric field parallel to the optic axis was found to be greater than the absorption for the electric field perpendicular to the optic axis and so the dichroism is said to be positive.

For low loss applications in the submillimeter, grade A possesses the most desirable properties. Its refractive index remains roughly constant over the frequency range studied and it exhibits the least absorption of the four grades studied (α < 1 cm^{-1} at frequencies $\leq$ 38 cm^{-1}). Its low cost, ability to be machined, and decreasing absorption into the millimeter region make h-BN an attractive material for applications such as windows and possibly waveplates.

CONCLUSION

Hexagonal Boron Nitride, a wide band gap insulator, has received recent attention in the millimeter/submillimeter spectral region due to its many desirable properties. Several grades of highly oriented polycrystalline BN with a predominantly hexagonal crystal were obtained from The Carborundum Company and their room temperature optical properties were studied from 18 cm^{-1} to 118 cm^{-1}. The refractive index n and absorption coefficient α were then determined

in this frequency region. The material was found to possess a measurable birefringence, and in some cases, exhibited a slight dichroic behavior. For low loss applications in the submillimeter, grade A appears to be the most desirable with the lowest absorption coefficient of the grades studied.

Table I   Birefringence and Dichroism at 100 cm^{-1} for three anisotropic insulators

material	crystal structure	$\Delta n = n_e - n_o$	$\Delta k = k_e - k_o$ (note: $\alpha = 4\pi k/\lambda$)
Boron nitride (*h*-BN), grade A	hexagonal	- 0.152	3×10^{-4}
Aluminum oxide (Al_2O_3)	rhombohedral	0.359	1×10^{-2}
Beryllium Oxide (BeO)	hexagonal	0.144	7×10^{-4}

REFERENCES

1. S.P.S. Arya and A. D'Amico, Thin Solid Films, **157**, 267 (1988)

2. C. Tarrio and S. E. Schnatterly, Phys. Rev B, **11**, 7852 (1989-I)

3. D. M. Hoffman, G. L. Doll and P. C. Eklund, Phys. Rev B, **30**, 6051 (1984)

4. H.P.R. Frederikse, A. H. Kahn, and A. L. Dragoo, J. Am Ceram. Soc., **68**, 131 (1985)

5. J. M. Dutta and C. R. Jones, J. Appl. Phys., **64**, 4674 (1988)

6. E. Hecht and A. Zajac, Optics (Addison-Wesley, 1974) Chap. 8

7. M Born and E. Wolf, Principles of Optics 6th edition (Pergamon Press, 1980), Chap. 14

8. E. D. Palik, editor, Handbook of Optical Constants of Solid II (Academic Press, Inc. 1991)

9. A. S. Barker, Phys. Rev., **132**, 1474 (1963)

10. E. Loh, Phys. Rev., **166**, 673 (1968)

Captions

Figure 1   Orientation of the Cartesian coordinate system to coincide with the

                  material's preferred axis and the arrangement of atoms

Figure 2a   Transmissivity (T) of Grade A as a function of frequency for $\vec{E}$ parallel to

                  the extraordinary (optic) axis

Figure 2b   Transmissivity (T) of Grade A as a function of frequency for $\vec{E}$ parallel to

                  the ordinary axis

Figure 2c   Transmissivity (T) of Grade M26 as a function of frequency for $\vec{E}$ parallel

                  to the extraordinary (optic) axis

Figure 2d   Transmissivity (T) of Grade M26 as a function of frequency for $\vec{E}$ parallel

                  to the ordinary axis

Figure 3a   Real part of the complex index of refraction for Grade A

Figure 3b   Real part of the complex index of refraction for Grade HP

Figure 3c   Real part of the complex index of refraction for Grade M

Figure 3d   Real part of the complex index of refraction for Grade M26

Figure 4a   Absorption coefficient for Grade A. The error bars for   are indicated in

                  the figure.

Figure 4b   Absorption coefficient for Grade HP. The error bars for   are indicated
                   in the figure.

Figure 4c   Absorption coefficient for Grade M. The error bars for   are indicated
                   in the figure.

Figure 4d   Absorption coefficient for Grade M26. The error bars for   are
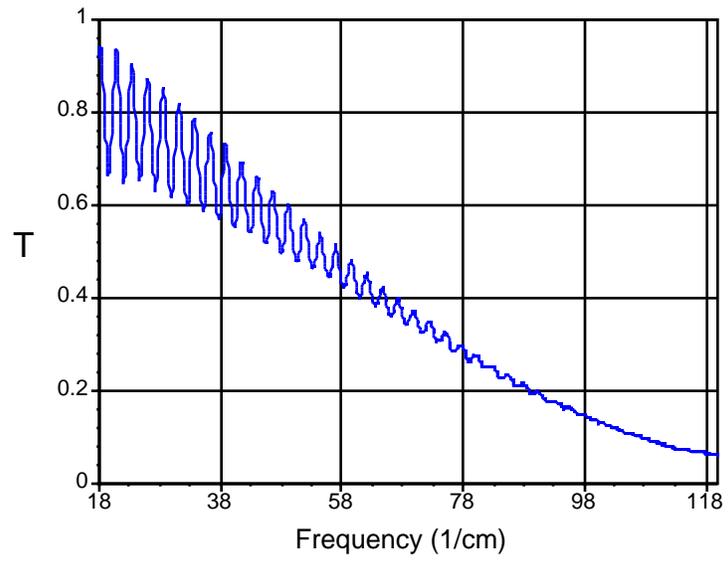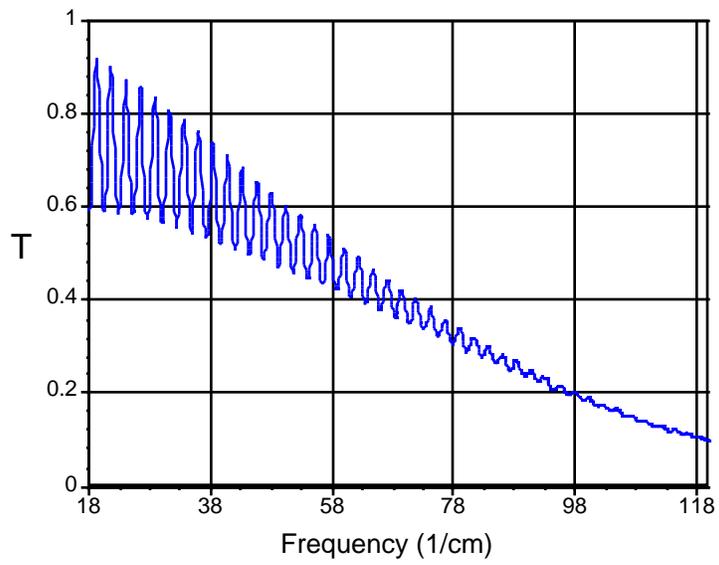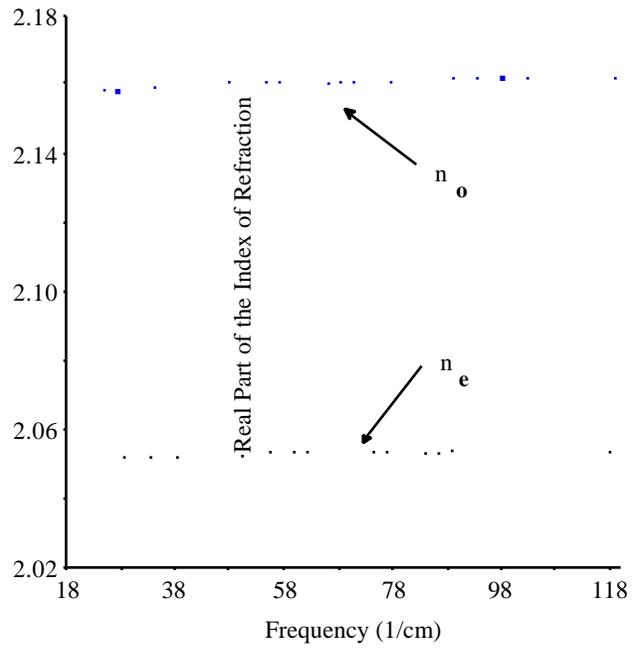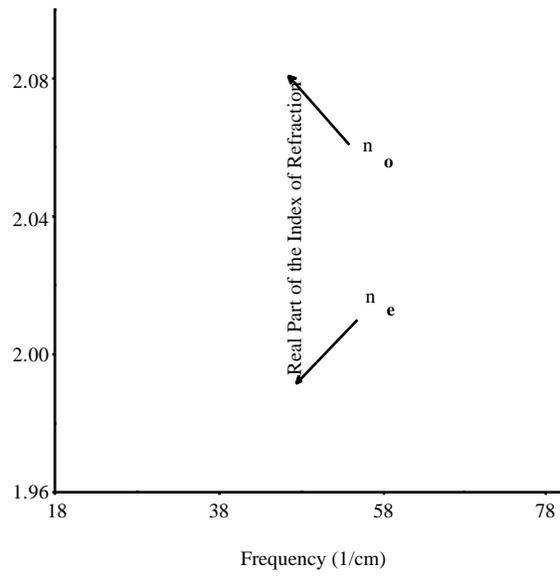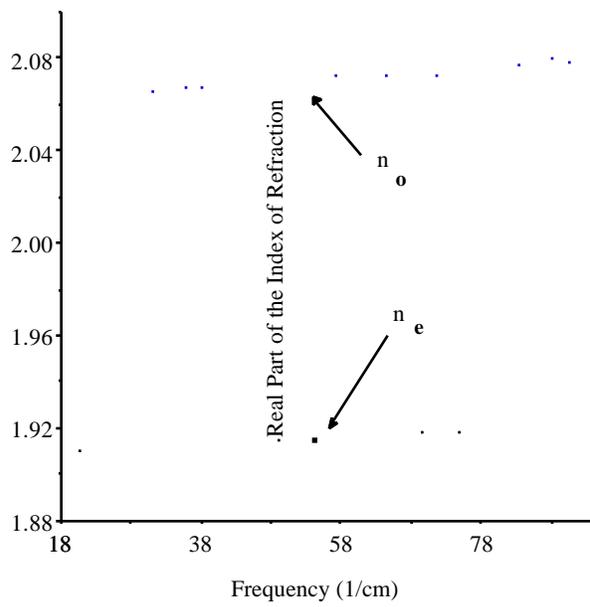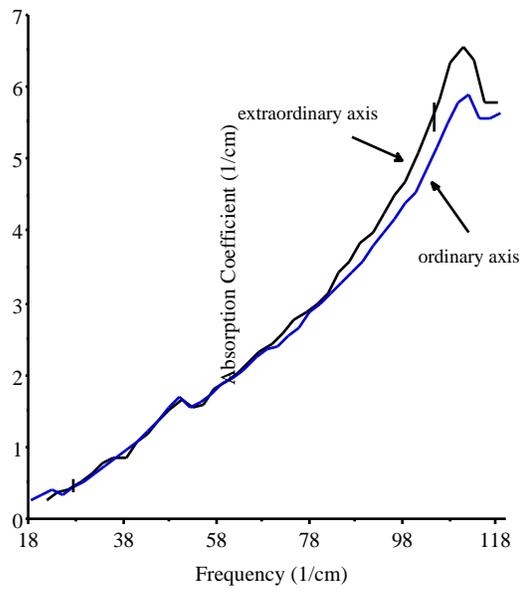   indicated in the figure.

planes of atoms
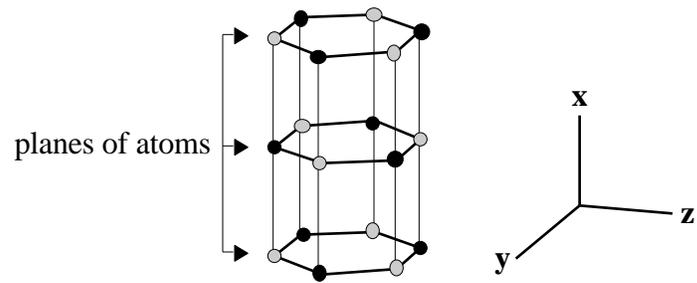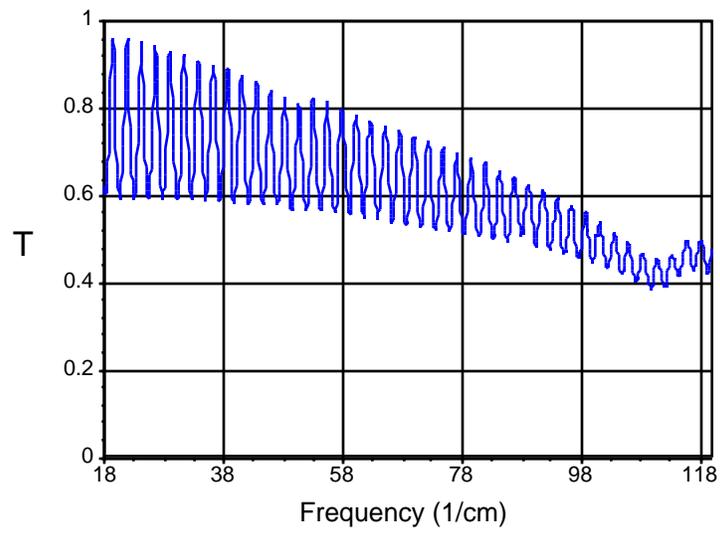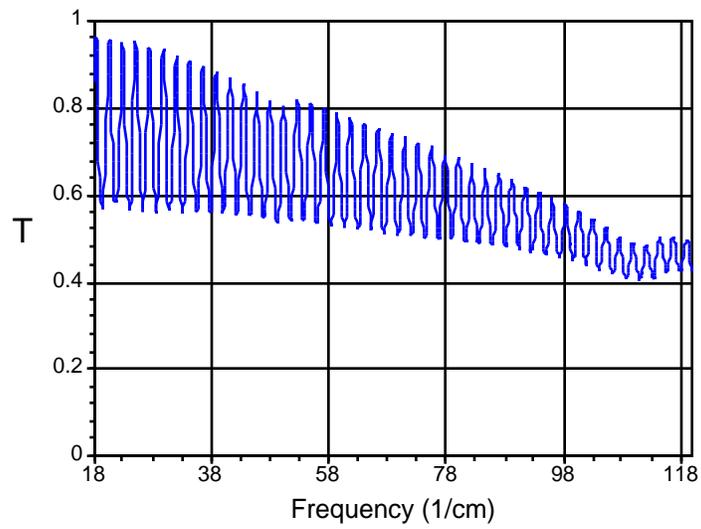
Figure 1

Figure 2a

Figure 2b
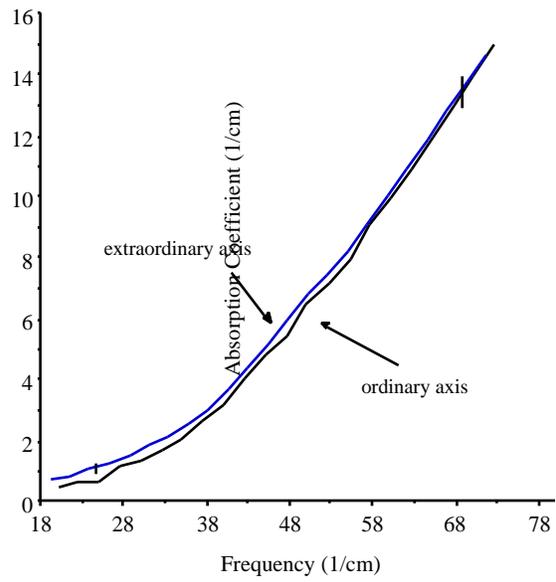
Figure 2c
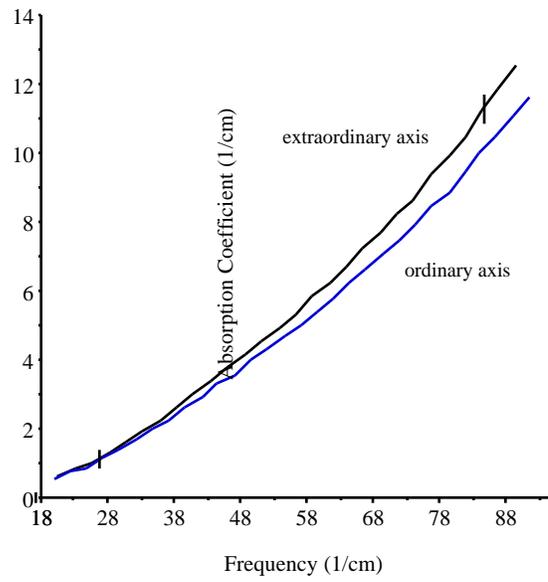

Figure 2d
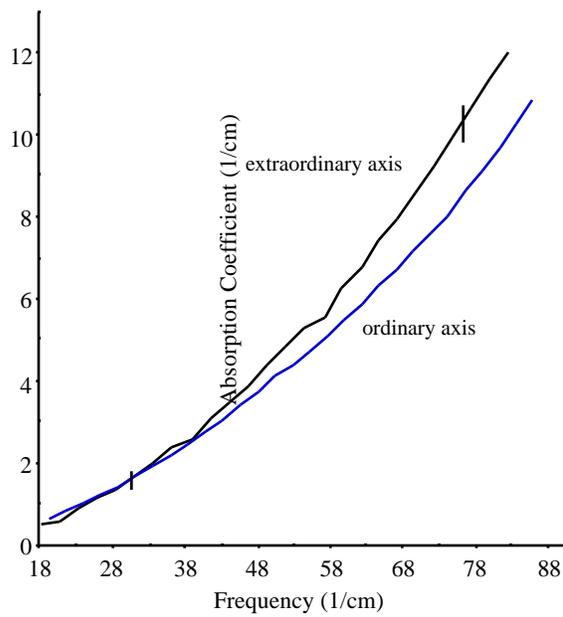
Figure 3a

Figure 3b
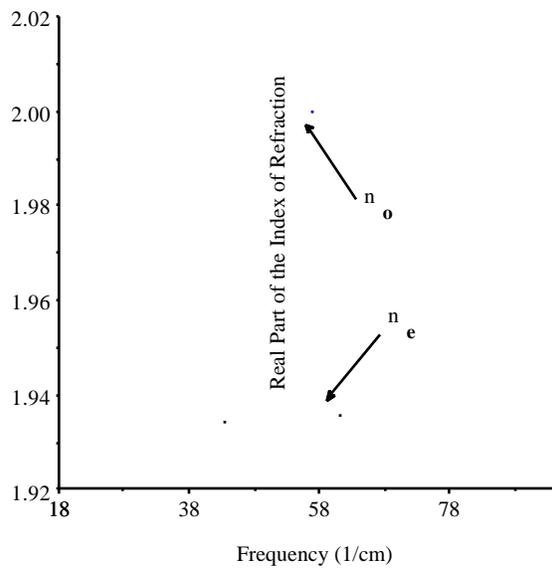
Figure 3c

Figure 3d

Figure 4a

Figure 4b

Figure 4c

Figure 4d